JOURNAL OF SPACECRAFT AND ROCKETS
Vol. 42, No. 6, November–December 2005

Spacecraft Rendezvous on Small Relative Inclination Orbits Using Tethers

Paul Williams*
Royal Melbourne Institute of Technology University, Melbourne, Victoria 3083, Australia

Tether-mediated rendezvous between a noncooperative payload and a maneuverable tether is considered. Practical scenarios in which the tether system orbit and payload are inclined relative to each other mean that capture is no longer limited to the orbital plane. The necessary conditions for achieving a zero position and zero velocity rendezvous when the tether system and payload are in arbitrary orbits are derived. Three case studies are considered in which the payload is inclined relative to the tether system by 0.5, 1.0, and 1.5 deg. Two direct transcription methods are used to obtain minimum reel acceleration trajectories for the system. It is shown that significant manipulation of the three-dimensional dynamics can be achieved in under two orbits using only tension control with smooth variations in tether length. A nonlinear receding horizon controller is considered for tracking the highly nonlinear system with disturbances to the system mass distribution and perturbations to the system initial conditions. Additional important considerations for payload capture are discussed.

Nomenclature

a = orbit semimajor axis, km
e = orbit eccentricity
i = orbit inclination, rad
L_f = fully deployed tether reference length, km
L_N = Nth-degree Legendre polynomial
l = tether length, km
m_t = tether mass, kg
m_2 = subsatellite mass, kg
R = orbit radius, km
T = tether tension, N
u = nondimensional control tension
θ = in-plane libration angle, rad
Λ = nondimensional tether length
μ = gravitational parameter, km^3/s^2
ν = orbit true anomaly, rad
ρ = tether line density, kg/km
ϕ = out-of-plane libration angle, rad
Ω = longitude of the ascending node, rad
ω = orbital angular velocity, rad/s
ϖ = argument of perigee, rad

Subscripts

p = payload
s = primary satellite

I. Introduction

TETHERED space systems have been proposed for a great number of applications.[1] Some example applications that have received considerable attention are deployment and retrieval of subsatellites,[2] aerobraking,[3] electrodynamic boost or deorbit of satellites,[4] and momentum transfer. Concepts involving propellantless momentum transfer are now well established. The most basic of these concepts involves either boosting or deorbiting a payload by means of a long tether. An example application of this is tether-assisted reentry,[5] in which optimal trajectories have been determined by several authors.[5–7] In this application, a payload is deployed along a controlled trajectory using a braking-only deployment mechanism so that the tether may be severed at the end of deployment, allowing the payload to reenter the Earth's atmosphere. Much more ambitious concepts have been proposed. Moravec[8] proposed using a rotating tether system, or nonsynchronous skyhook, that is designed to orbit a planet and touch the planet's surface with zero relative velocity. In this way, it would be possible to pick up and toss payloads into orbit. The use of tethers for momentum transfer in orbit was first considered by Colombo[9] and explored by Bekey[10] and Bekey and Penzo.[11] Tether deployment trajectories for a system in a circular orbit considering zero tension and full tension arcs were determined by Wiesel[12] to maximize the orbital energy of the payload at the release point. Kyroudis and Conway[13] considered the swinging release of payloads from tether systems in elliptical orbits. In their study, the tether is deployed with constant velocity and timed so that the tether passes through the local vertical on a forward swing during periapse passage, where the payload would be released. Tillotson[14] considered using spinning tethers to perform inclination changes for payloads in momentum exchange scenarios. In this proposal, the tether system is designed to spin perpendicularly to the orbital plane. Rendezvous maneuvers for this system have not currently been studied in detail. Forward[15] considered the possibility of transferring payloads from low Earth orbit (LEO) to the moon using tethers. This idea has since been expanded to consider systems for transferring payloads to Mars,[16] and several detailed studies have been performed for such systems.[16–19] Lorenzini et al.[20] analyzed a two-stage tether system for transferring payloads from LEO to geostationary orbit and concluded that the system is more competitive than chemical systems. Taylor[21] has discussed some of the major issues in conducting momentum exchange missions for boosting payloads from LEO to a geosynchronous transfer orbit and concluded that such systems will be more expensive than chemical rockets when factors such as atmospheric drag and orbital perturbations are taken into account. Ziegler and Cartmell[22] introduced the idea of using a symmetrical double-ended motorized tether for payload transfer. In their concept, the tether spin rate is controlled by a motor and tangential boosters on each of the payloads. With the exception of that of Tillotson,[14] all rendezvous scenarios that have been proposed ideally occur in the orbital plane.

There are several challenges that must be overcome before momentum-exchange systems can be made operational. One of the most critical aspects of the momentum-exchange techniques proposed in the literature is tether-mediated rendezvous and payload capture. This phase is by far the most critical and involves

Received 27 June 2004; presented as Paper 2004-5310 at the AIAA/AAS Astrodynamics Specialists Conference, Providence, RI, 16–19 August 2004; revision received 8 November 2004; accepted for publication 12 November 2004.

*Research Fellow, School of Aerospace, Mechanical, and Manufacturing Engineering. Student Member AIAA.

rather complicated dynamics. Tether-mediated orbital rendezvous was first mentioned by Carroll[23] for cooperative rendezvous between the tether tip and the space shuttle. Carroll[24] later provided a preliminary design for a tether transport facility capable of providing between 0.9- and 1.2-km/s velocity increments to payloads. In this work, a slowly spinning tether configuration is used, and techniques for mitigating the tension waves created by capturing and releasing payloads through tether reeling are discussed. Stuart[25] originally considered in-plane cooperative tether-mediated rendezvous between a free flying spacecraft and the tether tip by combining tether reeling with thrusters on the tether tip. In this work, however, the tether reel dynamics were not directly considered, and the nominal tether length was limited to 10 km. Stuart gave consideration to both minimum fuel and maximum rendezvous time trajectories. Maximum time trajectories were calculated by matching the tether tip and payload positions and velocities at an instant, and then setting the tether tension to near zero values maintained by thrusting along the tether line. More recently, Blanksby and Trivailo[26] devised a method for achieving a gentle rendezvous for the in-plane case using tension control. A simpler control technique was suggested by Williams et al.,[27] employing a nonlinear receding horizon tracking controller. In this approach, the tether tip is maneuvered from an arbitrary initial state to a unique libration cycle that ensures rendezvous at the rendezvous time. Westerhoff[28] discusses a linear control strategy to minimize errors in rendezvous for a spinning momentum-exchange system, assuming that the tether is positioned reasonably close to the desired rendezvous position. It is assumed that errors in the out-of-plane direction can be handled by thrusters on the payload.

In this paper, we consider the use of tethers for the capture of noncooperative payloads. Such a system is useful for applications such as debris removal. In these scenarios, it is unrealistic to assume that the orbital planes of the tether system and target payload will coincide. Rendezvous for the case in which there is a small relative inclination between the tether system and payload will require that capture occurs out of plane with respect to the tether system. This paper derives the necessary conditions for the position and velocity of the tether tip to ensure rendezvous. An optimal guidance strategy utilizing only tension control is suggested that minimizes the variation in the tether reel acceleration. Three examples are considered to illustrate the effectiveness of using only tension control to guide the system in the in- and out-of-plane directions in as few as two orbital revolutions. Feedback control is also considered using a receding horizon tracking control strategy.

II. Dynamic Model

To derive an open-loop trajectory for out-of-plane rendezvous requires a simple model of the tether that expresses the fundamental dynamics of the system. The model selected is shown in Fig. 1. It assumes that the tether is a rigid, massive link that may change in length via tension control at the primary satellite. The primary satellite is constrained to follow a circular orbit with radius R_s, angular rate ω_s, and true anomaly ν_s. The generalized coordinates for describing the motion of the tether are selected as the orthogonal polar coordinates l, θ, and ϕ, where l is the tether length, θ is the in-plane libration angle, and ϕ is the out-of-plane libration angle. The alignment of the tether is given by starting with the tether along the positive x axis, rotating by θ about the positive z axis (in-plane), and then rotating by ϕ about the rotated y axis (out-of-plane). The selected model is relatively simple, but provides a good first approximation to the motion of the tether tip and has been used widely for the design of control laws for the system, such as the Small Expendable Deployment System-II.[29]

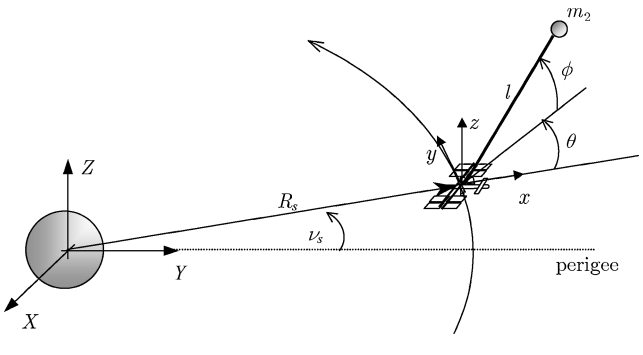

Fig. 1 Simplified tether model for design of control laws.

The equations of motion for a tether system in a reference circular orbit may be written as[7]

$$\theta'' = 2(\theta'+1)\left[\phi'\tan\phi - \left(\frac{m_2+m_t/2}{m_2+m_t/3}\right)\frac{\Lambda'}{\Lambda}\right] - 3\sin\theta\cos\theta \quad (1)$$

$$\phi'' = -2\left(\frac{m_2+m_t/2}{m_2+m_t/3}\right)\frac{\Lambda'}{\Lambda}\phi' - [(\theta'+1)^2 + 3\cos^2\theta]\sin\phi\cos\phi \quad (2)$$

$$\Lambda'' = -\frac{m_t}{2(m_2+m_t)}\frac{\Lambda'^2}{\Lambda} + \left(\frac{m_2+m_t/2}{m_2+m_t}\right)\Lambda \times [\phi'^2 + (\theta'+1)^2\cos^2\phi + 3\cos^2\theta\cos^2\phi - 1] - u \quad (3)$$

where $()' = \mathrm{d}/\mathrm{d}(\omega_s t)$ represents the nondimensional time derivative, $u = T/[(m_2+m_t)L_f\omega_s^2]$ is the nondimensional control tension, T is the tether control tension, Λ is the nondimensional tether length normalized with respect to the fully deployed tether length L_f, and m_t is given by

$$m_t = \rho\Lambda L_f \quad (4)$$

where ρ is assumed to be constant.

III. Out-of-Plane Rendezvous Conditions

In this section, equations that specify the terminal conditions for the tether tip for rendezvous with a payload in an arbitrary elliptical orbit are derived. Figure 2 shows the coordinate systems used to relate the position and velocity of the payload to the position and velocity of the tether tip. The Earth-centered inertial coordinate system (X, Y, Z) is attached to the center of the Earth and is used to calculate the inertial positions of the payload and tether tip. The orbital coordinates (x, y, z) are attached to the center of mass of the tether system and rotate so that the x axis is always aligned with the local vertical and parallel to the orbit radius vector. The y axis is tangential to the orbit, and the z axis points positively in the direction of the angular momentum vector of the tether system orbit.

Consider the motion of an arbitrary satellite about the Earth. In orbital coordinates, the radius vector can be written as

$$\boldsymbol{r}_i = \frac{a_i\left(1-e_i^2\right)}{1+e_i\cos\nu_i}\boldsymbol{i}_i \quad (5)$$

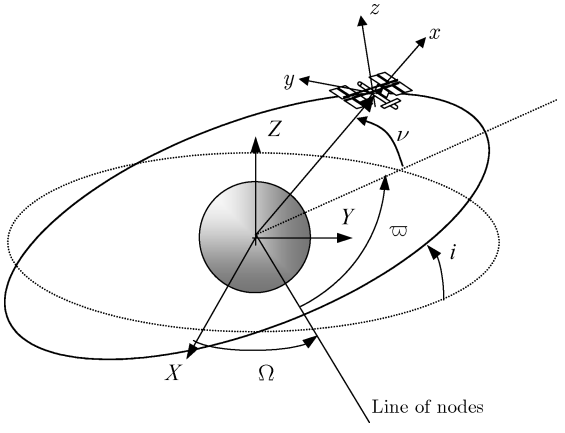

Fig. 2 Definition of coordinate systems used for rendezvous state determination.

where the subscript i is used to denote either the primary satellite s or the payload p. The velocity vector is also given by

$$\boldsymbol{v}_i = \sqrt{\mu/a_i\left(1-e_i^2\right)}e_i \sin\nu_i \boldsymbol{i}_i + \sqrt{\mu/a_i\left(1-e_i^2\right)}(1+e_i\cos\nu_i)\boldsymbol{j}_i \tag{6}$$

The orbital coordinates are related to the inertial coordinates by the orthogonal transformation

$$\begin{Bmatrix} \boldsymbol{X} \\ \boldsymbol{Y} \\ \boldsymbol{Z} \end{Bmatrix} = [C_i] \begin{Bmatrix} \boldsymbol{i}_i \\ \boldsymbol{j}_i \\ \boldsymbol{k}_i \end{Bmatrix} \tag{7}$$

where

$$C_i = \begin{bmatrix} c\Omega_i c(\varpi_i+\nu_i) - s\Omega_i s(\varpi_i+\nu_i)ci_i, & -c\Omega_i s(\varpi_i+\nu_i) - s\Omega_i c(\varpi_i+\nu_i)ci_i, & s\Omega_i si_i \\ s\Omega_i c(\varpi_i+\nu_i) + c\Omega_i s(\varpi_i+\nu_i)ci_i, & -s\Omega_i s(\varpi_i+\nu_i) + c\Omega_i c(\varpi_i+\nu_i)ci_i, & -c\Omega_i si \\ s(\varpi_i+\nu_i)si_i, & c(\varpi_i+\nu_i)si_i, & ci_i \end{bmatrix} \tag{8}$$

where $c(\,)$ and $s(\,)$ represent the cosine and sine functions, respectively. The position and velocity vectors of the tether system and payload may be written as

$$\boldsymbol{R}_i = [C_i]\boldsymbol{r}_i, \qquad \boldsymbol{V}_i = [C_i]\boldsymbol{v}_i \tag{9}$$

where the subscript $i = s$ means that the orbital elements of the tether system are substituted into Eq. (8) and similarly for the subscript $i = p$ for the payload. The relative position and velocity vectors of the tether system with respect to the payload in tether system orbital coordinates are given by

$$\begin{aligned} \boldsymbol{r}_{\text{rel}} &= [C_s]^\top(\boldsymbol{R}_p - \boldsymbol{R}_s) = [C_s]^\top[C_p]\boldsymbol{r}_p - \boldsymbol{r}_s \\ \boldsymbol{v}_{\text{rel}} &= [C_s]^\top(\boldsymbol{V}_p - \boldsymbol{V}_s) = [C_s]^\top[C_p]\boldsymbol{v}_p - \boldsymbol{v}_s \end{aligned} \tag{10}$$

It is possible to relate the expressions for $\boldsymbol{r}_{\text{rel}}$ and $\boldsymbol{v}_{\text{rel}}$ to the generalized coordinates by considering that the position of the tether tip relative to the tether platform in orbital coordinates is given by

$$\boldsymbol{r} = l\cos\theta\cos\phi\boldsymbol{i}_s + l\sin\theta\cos\phi\boldsymbol{j}_s + l\sin\phi\boldsymbol{k}_s \tag{11}$$

Taking the time derivative of Eq. (11) yields

$$\begin{aligned} \boldsymbol{v} = (&\dot{l}\cos\theta\cos\phi - l\dot{\theta}\sin\theta\cos\phi - l\dot{\phi}\cos\theta\sin\phi \\ &- l\omega_s\sin\theta\cos\phi)\boldsymbol{i}_s + (\dot{l}\sin\theta\cos\phi + l\dot{\theta}\cos\theta\cos\phi \\ &- l\dot{\phi}\sin\theta\sin\phi + l\omega_s\cos\theta\cos\phi)\boldsymbol{j}_s + (\dot{l}\sin\phi + l\dot{\phi}\cos\phi)\boldsymbol{k}_s \end{aligned} \tag{12}$$

The position and velocity of the payload may be determined in terms of the tether generalized coordinates by equating the components of Eqs. (10–12) and solving for the unknown variables. The spherical coordinates are calculated in a straightforward manner as

$$\Lambda = \sqrt{(\boldsymbol{r}_{\text{rel}}\cdot\boldsymbol{i}_s)^2 + (\boldsymbol{r}_{\text{rel}}\cdot\boldsymbol{j}_s)^2 + (\boldsymbol{r}_{\text{rel}}\cdot\boldsymbol{k}_s)^2}\Big/L_f \tag{13}$$

$$\theta = \text{atan2}(\boldsymbol{r}_{\text{rel}}\cdot\boldsymbol{j}_s, \boldsymbol{r}_{\text{rel}}\cdot\boldsymbol{i}_s) \tag{14}$$

$$\phi = \sin^{-1}[\boldsymbol{r}_{\text{rel}}\cdot\boldsymbol{k}_s/(\Lambda L_f)] \tag{15}$$

The nondimensional tether length and libration rates are calculated using the results from Eqs. (13–15) and equating the components of Eqs. (10) and (12),

$$\begin{bmatrix} \cos\theta\cos\phi & -l\sin\theta\cos\phi & -l\cos\theta\sin\phi \\ \sin\theta\cos\phi & l\cos\theta\cos\phi & -l\sin\theta\sin\phi \\ \sin\phi & 0 & l\cos\phi \end{bmatrix} \begin{bmatrix} \dot{l} \\ \dot{\theta} \\ \dot{\phi} \end{bmatrix}$$

$$= \begin{bmatrix} l\omega_s\sin\theta\cos\phi + \boldsymbol{v}_{\text{rel}}\cdot\boldsymbol{i}_s \\ -l\omega_s\cos\theta\cos\phi + \boldsymbol{v}_{\text{rel}}\cdot\boldsymbol{j}_s \\ \boldsymbol{v}_{\text{rel}}\cdot\boldsymbol{k}_s \end{bmatrix} \tag{16}$$

After solving the linear system of equations (16) and making use of the relationship between dimensional and nondimensional variables, that is, $\dot{l} = \Lambda' L_f\omega_s$, $\dot{\theta} = \theta'\omega_s$, and $\dot{\phi} = \phi'\omega_s$, one obtains

$$\begin{aligned} \Lambda' = &\left(\frac{\boldsymbol{v}_{\text{rel}}\cdot\boldsymbol{i}_s}{\omega_s L_f} + \Lambda\sin\theta\cos\phi\right)\cos\theta\cos\phi \\ &+ \left(\frac{\boldsymbol{v}_{\text{rel}}\cdot\boldsymbol{j}_s}{\omega_s L_f} - \Lambda\cos\theta\cos\phi\right)\sin\theta\cos\phi + \frac{\boldsymbol{v}_{\text{rel}}\cdot\boldsymbol{k}_s}{\omega_s L_f}\sin\phi \end{aligned} \tag{17}$$

$$\begin{aligned} \theta' = &-\left(\frac{\boldsymbol{v}_{\text{rel}}\cdot\boldsymbol{i}_s}{\omega_s\Lambda L_f} + \sin\theta\cos\phi\right)\frac{\sin\theta}{\cos\phi} \\ &+ \left(\frac{\boldsymbol{v}_{\text{rel}}\cdot\boldsymbol{j}_s}{\omega_s\Lambda L_f} - \cos\theta\cos\phi\right)\frac{\cos\theta}{\cos\phi} \end{aligned} \tag{18}$$

$$\begin{aligned} \phi' = &-\left(\frac{\boldsymbol{v}_{\text{rel}}\cdot\boldsymbol{i}_s}{\omega_s\Lambda L_f} + \sin\theta\cos\phi\right)\cos\theta\sin\phi \\ &- \left(\frac{\boldsymbol{v}_{\text{rel}}\cdot\boldsymbol{j}_s}{\omega_s\Lambda L_f} - \cos\theta\cos\phi\right)\sin\theta\sin\phi + \frac{\boldsymbol{v}_{\text{rel}}\cdot\boldsymbol{k}_s}{\omega_s\Lambda L_f}\cos\phi \end{aligned} \tag{19}$$

We consider three example rendezvous cases where the tether system and payload are in different altitude circular orbits. For simplicity, the following parameters are employed:

$$\begin{aligned} (a_s, e_s, i_s, \Omega_s, \varpi_s, \nu_{s_0}) &= (6{,}770{,}882\text{ m}, 0, 0, 0, 0, 0) \\ (a_p, e_p, \Omega_p, \varpi_p, \nu_{p_0}) &= (6{,}670{,}882\text{ m}, 0, 0, 0, -1\text{ rad}) \end{aligned} \tag{20}$$

with $i_p = 0.5$, 1.0, and 1.5 deg. The nominal tether length is selected to be $L_f = 100$ km, which would be the length required for an in-plane circular orbit rendezvous. In reality, capture will not take place with the tether exactly at this length due to out-of-plane capture requirements. Note that the method for open-loop guidance proposed in Sec. IV has been tested successfully for relative inclinations up to 5 deg, but requires tether lengths on the order of 300 km. For simplicity, and to allow comparisons between the three different cases for similar tether lengths, inclinations larger than 1.5 deg are not considered.

For coplanar orbits, assuming no orbital perturbations, there is a fixed amount of time between optimal rendezvous opportunities. An optimal rendezvous opportunity is defined to be one where the relative distance between the tether platform and payload is a minimum. By definition, these cases must occur when the relative velocity along the tether radial direction is zero. For the in-plane capture case, rendezvous is optimal when the tether is swinging in a retrograde swing at the instant when the tether is aligned along the local vertical. When the payload is inclined relative to the tether platform, there is no such unique rendezvous opportunity because the distance to the payload has multiple minima over many orbits. This is an important difference between the in-plane and out-of-plane rendezvous scenarios.

Table 1 shows the capture opportunities for a period of 30 days using the parameters defined earlier for three different relative inclinations. To reduce tether length requirements, a capture opportunity is defined to be when the tether length rate is zero and the tether length

Table 1 Rendezvous opportunities and required rendezvous conditions over a 30-day period for different relative inclination orbits

	0.5 deg			1.0 deg			1.5 deg		
Case	Time, days	Final conditions		Time, days	Final conditions		Time, days	Final conditions	
1	0.4521	θ	**−3.09798**	0.4513	θ	**−2.9614**	0.4507	θ	−2.8675
		θ'	**1.4973**		θ'	**−1.4471**		θ'	−1.3731
		ϕ	**0.1608**		ϕ	**0.2260**		ϕ	0.2232
		ϕ'	**0.5704**		ϕ'	**1.1466**		ϕ'	1.7015
		Λ	**1.0152**		Λ	**1.0436**		Λ	1.0663
		Λ'	**0**		Λ'	**0**		Λ'	0
2	3.2967	θ	3.0273	3.2988	θ	2.7371	3.3009	θ	2.5085
		θ'	−1.4840		θ'	−1.2634		θ'	−0.9607
		ϕ	0.3966		ϕ	0.5414		ϕ	0.4903
		ϕ'	−0.4066		ϕ'	−0.8994		ϕ'	−1.3207
		Λ	1.0929		Λ	1.2751		Λ	1.4165
		Λ'	0		Λ'	0		Λ'	0
3	6.1386	θ	−3.0347	6.1363	θ	−2.7144	8.9837	θ	2.9919
		θ'	−1.4867		θ'	−1.2386		θ'	−1.4491
		ϕ	−0.4441		ϕ	−0.6134		ϕ	−0.1236
		ϕ'	−0.3352		ϕ'	0.8010		ϕ'	1.7606
		Λ	1.1158		Λ	1.3519		Λ	1.0194
		Λ'	0		Λ'	0		Λ'	0
4	8.9829	θ	3.1075	8.9834	θ	3.0433	14.6664	θ	−2.7074
		θ'	−1.5013		θ'	−1.4808		θ'	−1.2185
		ϕ	−0.0870		ϕ	−0.1233		ϕ	−0.3449
		ϕ'	0.5882		ϕ'	1.1778		ϕ'	−1.5731
		Λ	1.0045		Λ	1.0127		Λ	1.1745
		Λ'	0		Λ'	0		Λ'	0
5	11.8264	θ	3.0936	14.6675	θ	−2.8560	17.5167	θ	2.6246
		θ'	−1.5008		θ'	−1.3763		θ'	−1.1181
		ϕ	0.5154		ϕ	−0.3599		ϕ	−0.4052
		ϕ'	−0.1274		ϕ'	−1.0734		ϕ'	1.4821
		Λ	1.1535		Λ	1.1156		Λ	1.2571
		Λ'	0		Λ'	0		Λ'	0
6	14.6689	θ	−3.0477	17.5153	θ	2.8032	23.1994	θ	−3.1034
		θ'	−1.4900		θ'	−1.3301		θ'	−1.4801
		ϕ	−0.2607		ϕ	−0.4319		ϕ	−0.0316
		ϕ'	−0.5258		ϕ'	1.0159		ϕ'	−1.7840
		Λ	1.0402		Λ	1.1705		Λ	1.0013
		Λ'	0		Λ'	0		Λ'	0
7	17.5136	θ	3.0348	20.3534	θ	−2.7397	28.8822	θ	**−2.5744**
		θ'	−1.4862		θ'	−1.2678		θ'	**−1.0521**
		ϕ	−0.3153		ϕ	0.7194		ϕ	**0.4417**
		ϕ'	0.4883		ϕ'	0.6151		ϕ'	**1.4176**
		Λ	1.0588		Λ	1.4565		Λ	**1.3187**
		Λ'	0		Λ'	0		Λ'	**0**
8	20.3558	θ	−3.0652	23.1995	θ	−3.1166	——	——	——
		θ'	−1.4953		θ'	−1.4943		——	——
		ϕ	0.4958		ϕ	−0.0314		——	——
		ϕ'	0.2116		ϕ'	−1.1897		——	——
		Λ	1.1428		Λ	1.0008		——	——
		Λ'	0		Λ'	0		——	——
9	23.1996	θ	−3.1328	26.0461	θ	2.7182	——	——	——
		θ'	−1.5029		θ'	−1.2435		——	——
		ϕ	−0.0221		ϕ	−0.6757		——	——
		ϕ'	−0.5948		ϕ'	0.6993		——	——
		Λ	1.0003		Λ	1.4161		——	——
		Λ'	0		Λ'	0		——	——
10	26.0437	θ	3.0501	28.8839	θ	−2.7726		——	——
		θ'	−1.4914		θ'	−1.3004	——	——	——
		ϕ	−0.4776		ϕ	0.4773		——	——
		ϕ'	0.2643		ϕ'	0.9720		——	——
		Λ	1.1331		Λ	1.2113		——	——
		Λ'	0		Λ'	0		——	——
11	28.8857	θ	−3.0295	——	——	——	——	——	——
		θ'	−1.4846		——	——		——	——
		ϕ	0.3498		——	——		——	——
		ϕ'	0.4582		——	——		——	——
		Λ	1.0724		——	——		——	——
		Λ'	0		——	——		——	——

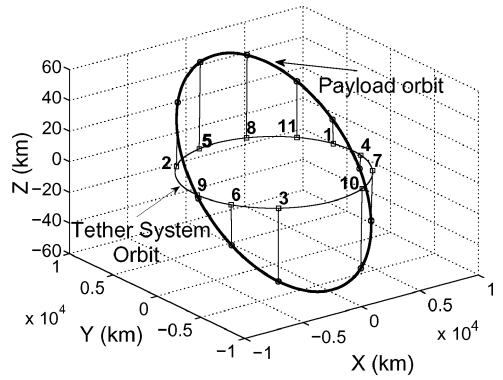

a) 0.5 deg

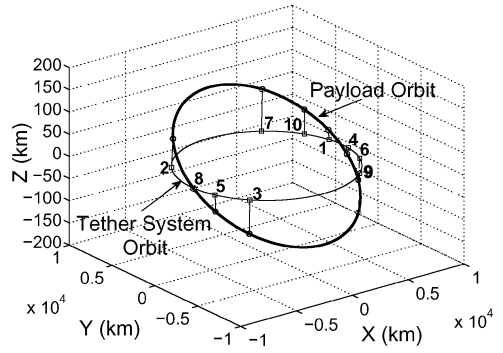

b) 1.0 deg

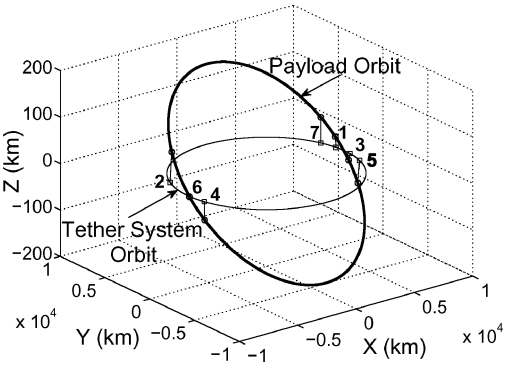

c) 1.5 deg

Fig. 3 Rendezvous opportunities.

is less than 1.5 times the nominal capture length L_f. Figure 3 shows the positions of the tether platform and payload, as well as the orientation of the tether. Note that the scaling on the axes is not the same. It is apparent from Table 1 that as the relative inclination of the orbit increases, opportunities for rendezvous become rarer, for example, compare 11 opportunities at 0.5-deg inclination with 7 opportunities at 1.5-deg inclination. This is a result of the constraint on maximum allowable tether length, which limits the excursion of the tether in the out-of-plane direction as the inclination increases. The maximum out-of-plane displacement of the payload increases with inclination (58.2 km for 0.5 deg, 116.4 km for 1.0 deg, and 174.6 km for 1.5 deg). For 0.5-deg inclination, rendezvous can occur at any point on the orbit given enough time to allow close proximity. However, for 1.5-deg inclination, opportunities for rendezvous tend to cluster around the point where the orbit planes intersect. The consequence of this is that the out-of-plane angle at rendezvous is decreased, and the out-of-plane libration rate must be correspondingly increased to match the velocity of the payload in the z direction. This effect can be seen by examining the required out-of-plane libration rates in Table 1 for 1.5-deg inclination and comparing them to the lower inclination cases. The particular cases selected for detailed study are boldfaced in Table 1, that is, one for each inclination.

IV. Open-Loop Guidance Algorithm

One of the main advantages of using space tethers for rendezvous and payload transfer is the propellant-free nature of the momentum-transfer concept. It is desirable to be able to manipulate the three-dimensional motion of the tether tip without expending propellant, or by limiting the use of propellant to correct errors in the trajectory. The objective of this section is to provide an approach for manipulating the motion of the tether tip in three dimensions using only tension control. This is quite a difficult task because the out-of-plane motion is coupled to the control variable Λ' only via nonlinear terms, as shown in Eq. (2). Note that tension is used to manipulate the length of tether, which affects the librational dynamics only via the Coriolis forces generated on the orbiting system.

The challenge is to find a physically realizable trajectory for the tether system that guides the tether tip from a given initial state to a fixed terminal state in a specified time. Such a problem is well-defined mathematically as a two-point boundary value problem. In general, there may be a finite number of trajectories that satisfy the boundary conditions, and, therefore, a numerical solution is not necessarily unique. It is preferable to enforce some additional measure of optimality for the trajectory, such as minimum energy or minimum control work. Although there are many possible measures for defining an optimal trajectory, in this paper the trajectory that satisfies the boundary conditions and that minimizes the integral square of the nondimensional tether reel acceleration is defined as optimal. Previous work has shown that such trajectories tend to give smoother variations in the system state variables, particularly the tether length and length rate, than those achieved by minimizing tension.[7] This is an important practical consideration that is often overlooked when designing optimal trajectories for tethered satellite systems. For example, Barkow et al.[30] obtain optimal deployment trajectories with a performance functional that minimizes the deviation of the libration angle from the local vertical. This results in a bang–bang optimal control problem for the control input (assuming an upper bound for the control tension). For control actuators such as thrusters, this may be acceptable; however, sudden changes in tension could lead to unwanted longitudinal and lateral vibrations of a flexible tether that could ultimately cause failure of the system. Furthermore, sudden changes in tension are often associated with rapid changes in the tether reel rate and could be difficult to achieve with practical reel mechanisms. A performance index that minimizes the tension rate might also help to prevent elastic oscillations of the tether. In fact, if the strain of the tether was included in the dynamics, then the strain rate should be minimized to suppress the tether elastic vibrations. However, because the tether is assumed to be inextensible, minimizing the tension rate does not produce smooth trajectories for the tether dynamics and is not employed here.

A. Optimal Control Problem

The control problem posed in this paper is to find the tension control input $u(t)$ that minimizes the performance index

$$\mathcal{J} = \int_{t_0}^{t_f} (\Lambda'')^2 \, \mathrm{d}t \tag{21}$$

subject to the dynamic constraints given by Eqs. (1–3), the initial and final boundary conditions

$$[\theta, \theta', \phi, \phi', \Lambda, \Lambda']_{t=t_0} = [\theta_0, \theta_0', \phi_0, \phi_0', \Lambda_0, \Lambda_0']$$

$$[\theta, \theta', \phi, \phi', \Lambda, \Lambda']_{t=t_f} = [\theta_f, \theta_f', \phi_f, \phi_f', \Lambda_f, \Lambda_f'] \tag{22}$$

as well as the box constraints

$$u_{\min} \leq u(t) \leq u_{\max} \tag{23}$$

where $u_{\min}$ is the lower bound on the nondimensional control tension, selected to prevent the tether from becoming slack, and $u_{\max}$ is the upper bound on the nondimensional control tension. In this work, $u_{\min} = 0.001$ and $u_{\max} = 40$.

A significant number of methods have been proposed[31] to solve problems of the form (or similar) defined by Eqs. (21–23). Among

them are shooting,[32] multiple shooting,[33] gradient,[34] conjugate-gradient,[35] and continuation methods.[36] These methods, often referred to collectively as indirect methods, suffer from the necessity of having to derive the necessary conditions for optimality via Pontryagin's maximum principle. In addition, initial estimates for the costates and jump conditions for problems with state inequalities are extremely difficult to obtain. Although no state inequalities are posed here, the control tension is extremely sensitive to errors, and this makes any method that employs direct integration of the state equations ill posed numerically. Furthermore, the well-known sensitivity of the costate equations adds another level of difficulty to the problem.

One way to overcome these difficulties is to employ direct transcription methods. Several such methods have become quite popular, including the Hermite–Simpson (see Refs. 37 and 38) and the Legendre pseudospectral method (see Refs. 39 and 40). The implementation of these methods are quite different and have been shown to produce different results under limited circumstances.[41] Because of this, both methods are used to obtain optimal trajectories for the system.

B. Direct Transcription Methods

Both the Hermite–Simpson and Legendre pseudospectral methods divide the time interval $t \in [t_0, t_f]$ into $N+1$ sequential node points. The spacing of the nodes is arbitrary for the Hermite–Simpson discretization, but is fixed in standard implementations of the Legendre pseudospectral discretization. In the following sections, the transcription methods are assumed to be transcribing problems of the basic form: Find the state-control pair $\{\boldsymbol{x}(t), \boldsymbol{u}(t)\}$ to minimize

$$\mathcal{J} = \mathcal{M}[x(t_f), t_f] + \int_{t_0}^{t_f} [\mathcal{L}(x(t), u(t), t)]\,\mathrm{d}t \tag{24}$$

subject to the state equations

$$\dot{\boldsymbol{x}}(t) = \boldsymbol{f}[\boldsymbol{x}(t), \boldsymbol{u}(t), t], \qquad t \in [t_0, t_f] \tag{25}$$

where $t \in \mathbb{R}$, $\boldsymbol{x}(t) \in \mathbb{R}^n$, $\boldsymbol{u}(t) \in \mathbb{R}^m$, $\mathcal{M} : \mathbb{R}^n \times \mathbb{R} \to \mathbb{R}$, and $\mathcal{L} : \mathbb{R}^n \times \mathbb{R}^m \times \mathbb{R} \to \mathbb{R}$.

1. Hermite–Simpson Discretization

The decision variables for the Hermite–Simpson discretization are the states and controls at the $N+1$ node points, together with the center controls (controls at the center of an interval), that is, $\boldsymbol{z} = \{\boldsymbol{x}_0, \boldsymbol{u}_0, \boldsymbol{v}_0, \ldots, \boldsymbol{v}_N, \boldsymbol{x}_N, \boldsymbol{u}_N\}$. The constraints are formulated by first using Hermite interpolation

$$\boldsymbol{y}_k = (\boldsymbol{x}_k + \boldsymbol{x}_{k+1})/2 + (h_k/8)[\boldsymbol{f}(\boldsymbol{x}_k, \boldsymbol{u}_k, t_k) - \boldsymbol{f}(\boldsymbol{x}_{k+1}, \boldsymbol{u}_{k+1}, t_{k+1})] \tag{26}$$

followed by Simpson quadrature, to satisfy the state equations

$$\boldsymbol{x}_k - \boldsymbol{x}_{k+1} + (h_k/6)\Big[\boldsymbol{f}(\boldsymbol{x}_k, \boldsymbol{u}_k, t_k) + 4\boldsymbol{f}_c\Big(\boldsymbol{y}_k, \boldsymbol{v}_k, t_{k+\frac{1}{2}}\Big) + \boldsymbol{f}(\boldsymbol{x}_{k+1}, \boldsymbol{u}_{k+1}, t_{k+1})\Big] = \boldsymbol{0} \tag{27}$$

for $k = 0, \ldots, N-1$, where $\boldsymbol{v}_k$ are the controls associated with the interval midpoint. Two cases may be distinguished: 1) where $\boldsymbol{v}_k$ is a free optimization variable, and 2) where $\boldsymbol{v}_k$ is determined by linear interpolation within an interval. To keep consistency in the number of optimization variables with the Legendre pseudospectral discretization, only the case where linear interpolation of the controls is used. The cost function is approximated as

$$\mathcal{J} \cong \mathcal{M}(\boldsymbol{x}_N, t_N) + \sum_{k=0}^{N-1} \frac{h_k}{6}\Big\{\mathcal{L}(\boldsymbol{x}_k, \boldsymbol{u}_k, t_k) + 4\mathcal{L}\Big(\boldsymbol{y}_k, \boldsymbol{v}_k, t_{k+\frac{1}{2}}\Big) + \mathcal{L}(\boldsymbol{x}_{k+1}, \boldsymbol{u}_{k+1}, t_{k+1})\Big\} \tag{28}$$

Note that there are ways that the nonlinear programming (NLP) problem can be altered in this method. One is to introduce additional variables representing $\boldsymbol{y}_k$ and to enforce Eq. (26) as an equality constraint. Another approach is to introduce an additional variable representing $\boldsymbol{f}_c(\boldsymbol{y}_k, \boldsymbol{v}_k, t_{k+1/2})$. The software OTIS uses the controls and their derivatives at the node points to form the Hermite interpolant to evaluate the control at the midpoint. For simplicity, the standard implementation of the discretization is used here.

2. Legendre Pseudospectral

The decision variables for the Legendre pseudospectral method are the states and controls at the nodes, that is, $\boldsymbol{z} = \{\boldsymbol{x}_0, \boldsymbol{u}_0, \ldots, \boldsymbol{x}_N, \boldsymbol{u}_N\}$. The nodes ξ_j are not defined arbitrarily but must correspond to the zeros of the derivative of the Nth-degree Legendre polynomial $L_N(\xi)$ in the interval $[-1, 1]$, including the endpoints. The nodes are transformed to the interval $[t_0, t_f]$ by the transformation

$$t = [(t_f - t_0)/2]\xi + (t_f + t_0)/2 \tag{29}$$

The state equations are then enforced as equality constraints by

$$\sum_{j=0}^{N} \mathcal{D}_{kj}\boldsymbol{x}_j - \left(\frac{t_f - t_0}{2}\right)\boldsymbol{f}(\boldsymbol{x}_k, \boldsymbol{u}_k, t_k) = \boldsymbol{0}, \qquad k = 0, \ldots, N \tag{30}$$

where

$$\mathcal{D}_{kj} = \begin{cases} [L_N(\xi_k)/L_N(\xi_j)][1/(\xi_k - \xi_j)], & k \neq j \\ -[N(N+1)/4], & k = j = 0 \\ N(N+1)/4, & k = j = N \\ 0, & \text{otherwise} \end{cases} \tag{31}$$

The cost function is approximated by a Gauss–Lobatto rule

$$\mathcal{J} \cong \mathcal{M}(\boldsymbol{x}_N, t_N) + \left(\frac{t_f - t_0}{2}\right)\sum_{k=0}^{N} w_k \mathcal{L}(\boldsymbol{x}_k, \boldsymbol{u}_k, t_k) \tag{32}$$

where

$$w_k = [2/N(N+1)]\{1/[L_N(\xi_k)]^2\}, \qquad k = 0, \ldots, N \tag{33}$$

Note the difference between the Legendre pseudospectral discretization method and the Hermite–Simpson discretization method. The Legendre pseudospectral method approximates the states and controls with Nth-degree polynomials over the entire time domain. Hence, the value of the states at one node directly impacts the derivative of the states at all other nodes. This has advantages from the point of view of providing spectral accuracy, but it also leads to dense Jacobian blocks along the main diagonal of the Jacobian. One major disadvantage is that functions that exhibit sharp discontinuities such as bang–bang controls cannot be captured with high accuracy. One approach that overcomes some of these difficulties is the pseudospectral knotting method. In this method, the global domain is divided into n_d smaller subdomains, each with order N_{n_d} approximating polynomials. The boundary conditions are implemented using knotting conditions depending on whether the state variables remain continuous or discontinuous within each phase. The pseudospectral knotting method is not considered in this paper.

C. Application of Direct Transcription to Tether-Assisted Rendezvous

The sensitivity of the tether dynamics to the control tension makes direct application of a collocation method difficult. For example, by the use of a similar method as that used by Josselyn and Ross[42] to verify the feasibility of the solution, if the interpolated controls from a direct transcription method are integrated with the tether equations of motion, it is often the case that the integrated solution diverges drastically from the collocation solution. (This is illustrated in the numerical results.) This is particularly true for retrieval scenarios and cases where the control tension changes rapidly. This is a result of the sensitivity of the control tension and not due to convergence of the discretization method. The only recourse in direct transcription methods is to use a greater number of discretization points. However,

an efficient guidance algorithm must be able to give reasonably accurate solutions without the need for an extremely large number of nodes. In some previous work on tether optimal control,[7,43] it has been shown that it is possible to maintain high accuracy by altering the optimization variable from the nondimensional tension u to use the nondimensional commanded length Λ_c. To achieve this, it is necessary to parameterize the tension as follows:

$$u = u_0 + k_1(\Lambda - \Lambda_c) + k_2\Lambda' \tag{34}$$

where u_0 is the tension for zero length acceleration for $k_1 = k_2 = 0$, and k_1 and k_2 are control gains. This form of tension input is selected because the tether length tends to stabilize around the commanded length with a damping ratio k_2. Note that Eq. (34) is not selected for any other reason than providing a more accurate form of control input in the form of a commanded length for the optimal control problem. In effect, it simplifies the tether length dynamics (assuming an unsaturated tension input) to

$$\Lambda'' + k_2\Lambda' + k_1\Lambda = k_1\Lambda_c \tag{35}$$

Equation (35) is the equation for a forced damped harmonic oscillator. The tension input is used for the generation of the open-loop path, but it also provides an inherent feedback quality that allows for errors due to discretization. More complicated expressions for the form of the tension input could be used, such as those involving nonlinear terms of the out-of-plane angle, as used by Monshi et al.[44] However, Monshi et al.[44] deal only with feedback control of the system and not with the optimal length modulation to effect significant and accurate changes to the three-dimensional motion of the tether tip. It will be demonstrated that Eq. (35) is sufficient for manipulating the motion of the tether in three dimensions.

Equation (34) is not implemented directly because it introduces a highly nonlinear path constraint compared to simply employing box constraints for the tension input. Instead, the commanded length Λ_c is determined from Eq. (34) using the converged values of the state and control variables from the NLP. This approach allows different control gains to be used without solving the control problem again.

D. Some Issues in Solving the Optimal Control Problem

1. NLP Solver

It is known that the computational performance of direct transcription methods can be affected by the NLP solver.[45] Because of the unavailability of the solver SPRNLP used by the software SOCS,[46] the widely used solvers NPSOL and SNOPT were considered. SNOPT[47] is selected over NPSOL because SNOPT is capable of solving much larger problems more efficiently than NPSOL, without supplying derivative information.

2. Initial Guess

One of the drawbacks of using gradient-based optimization methods is that they can be susceptible to local minima. In general, convergence is dependent on the initial guess provided for the states and controls. Naturally, it is desirable to obtain global minima rather than local minima. The convergence of the problem studied in this paper has been found to be strongly dependent on the initial guess. For example, for in-plane motion, the equilibrium configuration for the tether provides a relatively good guess for the trajectory. However, for the cases in this paper, this is an extremely poor guess.

The method used by SOCS is to provide trajectories that vary linearly between the prescribed boundary conditions. One method to generate feasible guesses for the state trajectory is to guess the control trajectory and propagate the state equations using a high-order Runge–Kutta propagator (ode45 in MATLAB®). This has the advantage that the initial trajectory satisfies the state equality constraints, but it does not necessarily satisfy the boundary conditions.

To generate trajectories that satisfy the boundary conditions, a homotopy process can be used. Because it is not known a priori that a solution exists for a given optimal control problem, it is necessary to modify the original optimal control problem. Let the desired terminal states be denoted by $\boldsymbol{x}_d$. The initial guess used in the homotopy approach is obtained by integrating the system equations forward from the known initial state with the tether length held fixed. This gives a set of initial terminal states $\boldsymbol{x}_n$. The discretized problem is then solved by perturbing the terminal state in a discrete manner as a function of the homotopy parameter σ as follows:

$$\boldsymbol{x}_f = (\boldsymbol{x}_d - \boldsymbol{x}_n)\sigma + \boldsymbol{x}_n, \qquad \sigma \in [0, 1] \tag{36}$$

The method used in this paper is to impose hard constraints on the terminal position and penalize the terminal velocities by setting the cost function as

$$\mathcal{J} = [\theta'(t_f) - \theta'_f]^2 + [\phi'(t_f) - \phi'_f]^2 + [\Lambda'(t_f) - \Lambda'_f]^2 \tag{37}$$

Once a feasible solution is obtained, the original problem is then solved. The homotopy parameter is incremented in steps of 0.1.

V. Feedback Control Algorithm

The preceding section presented an approach for determining an open-loop optimal path to maneuver the tether tip from a given set of initial conditions to a final terminal state. Inevitably, there will be errors due to modeling, initial conditions, and external disturbances that have not been accounted for. These disturbances to the system need to be controlled by an appropriate means. One approach is to employ a neighboring optimal feedback controller based on the linearized state and costate dynamics around the optimal trajectory. This is equivalent to minimizing the second variation of the cost function along the optimal trajectory and is discussed in detail by Bryson.[48] Most algorithms for implementing neighboring optimal feedback control are based on backward sweep methods or involve constructing transition matrices. In contrast, Yan et al.[49] present a method for generating neighboring optimal paths using pseudospectral methods. In their approach, the linear differential equations of the auxiliary minimum problem are discretized using a pseudospectral method that effectively converts the differential equations to a set of linear algebraic equations. The boundary conditions for the auxiliary minimum problem are incorporated via matrix partitioning, and the set of equations are solved by a least-squares algorithm. In a similar vein, Williams[50] adapted the approach of Yan et al.[49] to the solution of nonlinear receding horizon control problems by combining pseudospectral discretization with a quasilinearization algorithm. Several problems involving tethered satellites were solved in Ref. 27 using a Chebyshev pseudospectral method, whereas retrieval of a subsatellite using a flexible tether is dealt with in Ref. 50 using a more general Jacobi pseudospectral discretization. A brief overview of the method is given next.

Consider the nonlinear receding horizon control problem of finding the control input $\boldsymbol{u}(t)$ that minimizes the performance index

$$\mathcal{J} = \frac{1}{2}[\boldsymbol{M}_f\boldsymbol{x} - \boldsymbol{\psi}]^\top \boldsymbol{S}_f[\boldsymbol{M}_f\boldsymbol{x} - \boldsymbol{\psi}]|_{t+T} + \frac{1}{2}\int_t^{t+T} \times \left\{ \begin{bmatrix} (\boldsymbol{x} - \boldsymbol{x}_d)^\top & (\boldsymbol{u} - \boldsymbol{u}_d)^\top \end{bmatrix} \begin{bmatrix} \boldsymbol{Q} & \boldsymbol{N} \\ \boldsymbol{N}^\top & \boldsymbol{R} \end{bmatrix} \begin{bmatrix} (\boldsymbol{x} - \boldsymbol{x}_d) \\ (\boldsymbol{u} - \boldsymbol{u}_d) \end{bmatrix} \right\} \mathrm{d}\tau^* \tag{38}$$

subject to the state equations and initial conditions

$$\dot{\boldsymbol{x}} = \boldsymbol{f}[\boldsymbol{x}(\tau^*), \boldsymbol{u}(\tau^*), \tau^*], \qquad \boldsymbol{x}(\tau^* = t) = \boldsymbol{x}(t) \tag{39}$$

where $\boldsymbol{x}(\tau^*) \in \mathbb{R}^n$ is the state vector, $\boldsymbol{x}_d(\tau^*) \in \mathbb{R}^n$ is the desired state vector, $\boldsymbol{u}(\tau^*) \in \mathbb{R}^m$ is the vector of control inputs, $\boldsymbol{u}_d(\tau^*) \in \mathbb{R}^m$ is the desired control input, $t \in \mathbb{R}$ is the time, $\tau^* \in [t, t+T] \in \mathbb{R}$ is the time variable used to predict the future system state $\boldsymbol{\psi} \in \mathbb{R}^p$, $p \leq n$ is the desired vector of values for the linear combination of desired final states $[\boldsymbol{M}_f\boldsymbol{x}(t+T)]$, $\boldsymbol{Q}$ is a positive-semidefinite matrix, $\boldsymbol{N}$ is a given matrix, $\boldsymbol{R}$ is a positive-definite matrix, $\boldsymbol{S}_f$ is the positive-semidefinite terminal weighting matrix, $\boldsymbol{M}_f$ is a given matrix, and

T is the length of the future horizon. Note that there is a distinction between the state and control variables used for predicting the future state, parameterized by τ^*, and the actual state and control variables, parameterized by t. Once the problem defined by Eqs. (38) and (39) is solved, the actual control input is applied at the current time by $\boldsymbol{u}(t) = \boldsymbol{u}(\tau^* = t)$.

The problem posed by Eqs. (38) and (39) is solved by applying quasi linearization to the system state equations, followed by formulating the necessary conditions for an optimal control via Pontryagin's maximum principle. Solutions may be obtained by discretizing the resulting set of linear equations via a pseudospectral method and incorporating the boundary conditions by eliminating the discretized equations at the boundaries. The method of quasi linearization requires that suitable guesses for the states and controls are provided. For tracking problems, these can simply be selected as the reference trajectories. The actual control input is determined by iterating on the sequence of the two-point boundary value problem obtained from the method of quasi linearization. Exact details of the implementation can be found in Ref. 50.

To apply the receding horizon controller to the tracking control of the tethered system in three dimensions, an additional control actuator is introduced. We assume that a thruster is available for producing a control force in the out-of-plane direction. This is not strictly necessary, but it makes the control algorithm more robust. Because it is desirable to limit propellant expenditure, the penalty term on the thruster usage is set to be relatively large. In any case, the main portion of the control work is achieved via tension control from the open-loop guidance algorithm, and so the requirements from the out-of-plane thruster are expected to be small.

The system equations for the tracking controller may be written as

$$\theta'' = 2(\theta' + 1)\left[\phi' \tan\phi - \left(\frac{m_2 + m_t/2}{m_2 + m_t/3}\right)\frac{\Lambda'}{\Lambda}\right] - 3\sin\theta\cos\theta \quad (40)$$

$$\phi'' = -2\left(\frac{m_2 + m_t/2}{m_2 + m_t/3}\right)\frac{\Lambda'}{\Lambda}\phi' - [(\theta' + 1)^2 + 3\cos^2\theta] \times \sin\phi\cos\phi + u_2 \quad (41)$$

$$\Lambda'' = -k_1(\Lambda - u_1) - k_2\Lambda' \quad (42)$$

where u_1 is the commanded length used for tracking control, $u_2 = F/[(m_2 + m_t/3)\omega_s^2 L_f]$ is the nondimensional out-of-plane thrust control input, F is the applied thrust, and k_1 and k_2 are the same control gains used in calculating the nominal trajectories. Equation (42) is subject to the constraint on the tether tension

$$k_1(\Lambda - u_1) + k_2\Lambda' + \left(\frac{m_2 + m_t/2}{m_2 + m_t}\right)\Lambda[\phi'^2 + (\theta' + 1)^2\cos^2\phi + 3\cos^2\theta\cos^2\phi - 1] - \frac{m_t}{2(m_2 + m_t)}\frac{\Lambda'^2}{\Lambda} \geq u_{\min} \quad (43)$$

where $u_{\min}$ is set to 0.001. When the control is violated at time t, the actual control input is clipped at the lower limit by choosing u_1 such that Eq. (43) is satisfied on the bound.

VI. Numerical Results

The open-loop optimal control problem is solved with initial conditions

$$\{\theta, \theta', \phi, \phi', \Lambda, \Lambda'\}_{t=0} = \{-\pi, 0, -20\,\text{deg}, 0, 1, 0\}$$

that are selected so that some out-of-plane motion is present in the system. It is well known that the out-of-plane motion cannot be excited by the in-plane motion without some disturbance to the out-of-plane dynamics, as indicated by Eq. (2). For this reason, an initial out-of-plane deflection is given. Such an initial state could be initiated during deployment of the tether or by electromagnetics. The final time is selected as $t_f = 12$ rad, which is slightly less than the time required for two orbital revolutions of the primary satellite. This is quite a short duration to manipulate the long period librational dynamics to meet a desired terminal state. It is selected for demonstrative purposes to show that only a small lead time is necessary to control the system satisfactorily. For determination of the open-loop control, the subsatellite mass is assumed to be 300 kg, but for closed-loop simulations it is taken to be 500 kg. The mass per unit length of tether is assumed to be 1 kg/km, with a reference length of $L_f = 100$ km.

Solutions are obtained in MATLAB 6.5 using SNOPT as the optimization software. Derivatives are provided by finite differences and take advantage of the sparsity patterns for the two discretization methods. Numerical results were obtained for the three different inclinations using different initial guesses. The results for the cost function values are listed in Table 2. Table 2 shows that the Hermite–Simpson discretization consistently converges to a lower minimum than the pseudospectral discretization, except for the 1.5-deg case when the homotopy method is used. There is some variation in the final results, depending on the discretization and the method used to generate the initial guess. It appears that the Hermite–Simpson method is more robust in converging than the pseudospectral method for this problem. This can be seen more clearly by comparing the results obtained from the pseudospectral method with the initial guess provided by the Hermite–Simpson method. This generates the lowest combined cost function values for each of the inclination cases for the pseudospectral discretization. In the results that follow, the results are taken from the bootstrapped Hermite–Simpson method for 100 nodes.

To show the effect of discretization error on tension control, Fig. 4 compares the propagated trajectory (ode45 in MATLAB) using the interpolated control input directly, with the propagated trajectory using the commanded tension [from Eq. (34)]. It is evident that, after approximately 6 rad, the propagated trajectory using tension diverges from the collocation solution, but the commanded tension trajectory remains accurate.

Figures 5–8 show the optimal open-loop trajectories together with closed-loop trajectories generated with the receding horizon

Table 2 Optimal cost function for open-loop rendezvous control

		Pseudospectral			Hermite–Simpson		
Initial guess method	Nodes	0.5 deg	1.0 deg	1.5 deg	0.5 deg	1.0 deg	1.5 deg
Homotopy[a]	100	0.1512	0.2844	0.8888	0.1074	0.2822	1.1475
Bootstrap[b]	20	——[c]	——	——	0.5561	0.7223	1.6972
Bootstrap	60	0.1911	0.4282	0.7909	0.1092	0.2862	0.7870
Bootstrap	100	0.1512	0.3352	0.7823	0.1074	0.2822	0.7776
HS[d]	100	0.1169	0.2844	0.7823	N/A	N/A	N/A

[a]System equations are integrated from initial conditions, and homotopy is used on the terminal boundary conditions to generate a feasible trajectory.
[b]Guess for state trajectories are straight lines between initial and final conditions. The control input is assumed zero. Bootstrapping from 20 nodes.
[c]Did not converge in 500 major iterations.
[d]Guess provided by best converged Hermite–Simpson result.

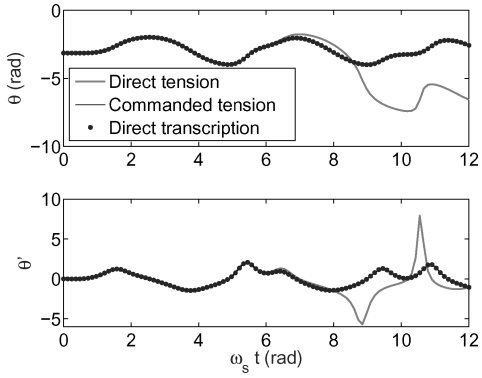

a) In-plane

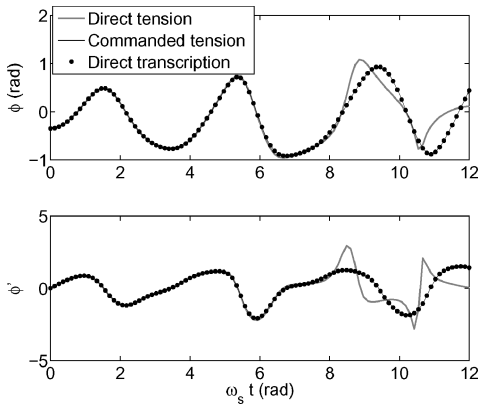

b) Out-of-plane

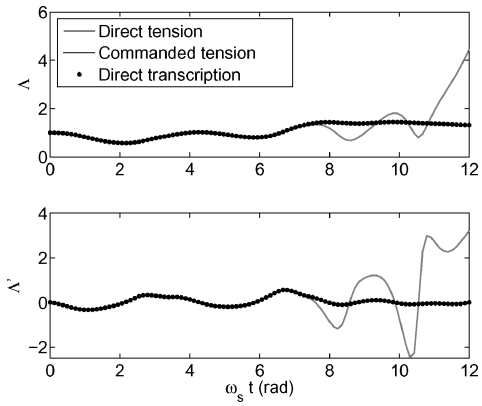

c) Length

Fig. 4 Comparison of using tension control input vs commanded tension control input for 1.5 deg.

tracking controller with the following properties:

$$\boldsymbol{Q} = \boldsymbol{S}_f = \begin{bmatrix} 10 & 0 & 0 & 0 & 0 & 0 \\ 0 & 10 & 0 & 0 & 0 & 0 \\ 0 & 0 & 50 & 0 & 0 & 0 \\ 0 & 0 & 0 & 30 & 0 & 0 \\ 0 & 0 & 0 & 0 & 40 & 0 \\ 0 & 0 & 0 & 0 & 0 & 10 \end{bmatrix} \tag{44}$$

$$\boldsymbol{R} = \begin{bmatrix} 500 & 0 \\ 0 & 500{,}000 \end{bmatrix} \tag{45}$$

The horizon length is selected as $T = 2$ rad, and 30 nodes are used on the prediction horizon. The controller is implemented at sampling times of 0.01 rad, which equates to approximately 10 s in real time. The disturbance given to the initial conditions is

$$\Delta \boldsymbol{x}_0 = [7\,\text{deg}, 0.1, 6\,\text{deg}, -0.05, 0.04, 0]^\top$$

Note that different combinations of control weightings, horizon length, and discretization level will give different results. The objective of the current study is not to provide a comprehensive study of the effect of such parameters, but rather to demonstrate the closed-loop control of the system.

Figure 5 shows the tether dynamics during open- and closed-loop control of the 0.5-deg relative inclination rendezvous case. Note that the tether must be reeled in by approximately 55% during the first orbit of the maneuver and then subsequently deployed to achieve the length required for rendezvous. This is a large variation in tether length, but it is necessary to effect the required changes in all three dimensions of the tether tip. The reeling requirements could possibly be reduced by allowing additional orbits to manipulate the motion. The length rate for the open-loop control shows a very smooth variation, which is the result of minimizing the square of the length acceleration. The closed-loop control shows some faster variations in tether length rate superimposed over the open-loop trajectory during the first orbit. The peak reel rate for the open-loop maneuver is on the order of 30 m/s, which increases to approximately 40 m/s in the closed-loop case. One of the effects of tether reeling is to produce in-plane librations of increasing amplitude. There is a peak in the tether libration rate at $\tau = \omega_s t \approx 5$ rad, corresponding to an in-plane swing rate of 0.152 deg/s. The out-of-plane dynamics are simultaneously pumped by the tether reeling. Note the significant increase in the out-of-plane angle during the first orbit. Also note that the closed-loop control is very effective at tracking all six state variables and that the closed-loop trajectory converges to the open-loop trajectory after approximately one orbit.

Figure 6 shows the open- and closed-loop trajectories for 1.0-deg relative inclination. In this case, the tether is reeled in by approximately 43% during the first orbit, which is significantly less (12 km) than the 0.5-deg inclination case. The peak reel-rate requirement is slightly higher than the 0.5-deg case (35 m/s compared to 30 m/s), and the reel rate has more variation in general. The peaks in reel rate occur in similar locations to the peaks in reel rate for the 0.5-deg case. After $\tau \approx 8$ rad the reel-rate requirements become minimal ($\sim$5 m/s), corresponding to the relatively flat period in the tether length toward the end of the maneuver. The in-plane librations are characterized by larger oscillations than the 0.5-deg case, although they do not appear to be growing with time. The in-plane libration rate is considerably different than the preceding case and exhibits more peaks, although the maximum peak is slightly less (0.13 deg/s). The out-of-plane librations are also quite different for this case, showing larger oscillations during the second orbit. This is a consequence of the larger out-of-plane rate required for rendezvous. Closed-loop control for this case is still very effective, but it causes the peak reel rate to increase to approximately 55 m/s very near the initial time. Tracking of all state variables converges at $\tau \approx 8$ rad.

Figure 7 shows the open- and closed-loop trajectories for 1.5-deg relative inclination. The dynamics for this case show some similarities to the 1.0-deg case, despite the significantly different rendezvous conditions. There are, however, some key differences that should be pointed out. The peak reel rate for this case is considerably higher (63 m/s compared to 35 m/s). This is necessary to achieve the final length constraint, which is almost 30 km larger than that in the preceding cases. Although the tether is reeled in by an identical amount to the 1.0-deg case, there is a much larger variation in length rate during the first orbit. The in-plane librations, although qualitatively similar to the 1.0-deg case, are larger in amplitude during most of the maneuver. The pumping of the out-of-plane dynamics is also similar, but increases toward the final time because of the higher out-of-plane angle and out-of-plane rate required for rendezvous. The closed-loop trajectory illustrates that this case is more difficult to track with the receding horizon controller, and convergence of all states to the open-loop trajectory is not achieved until $\tau \approx 11$ rad.

Figure 8 shows the tension control input for each case, together with the out-of-plane thruster requirements. The results illustrate

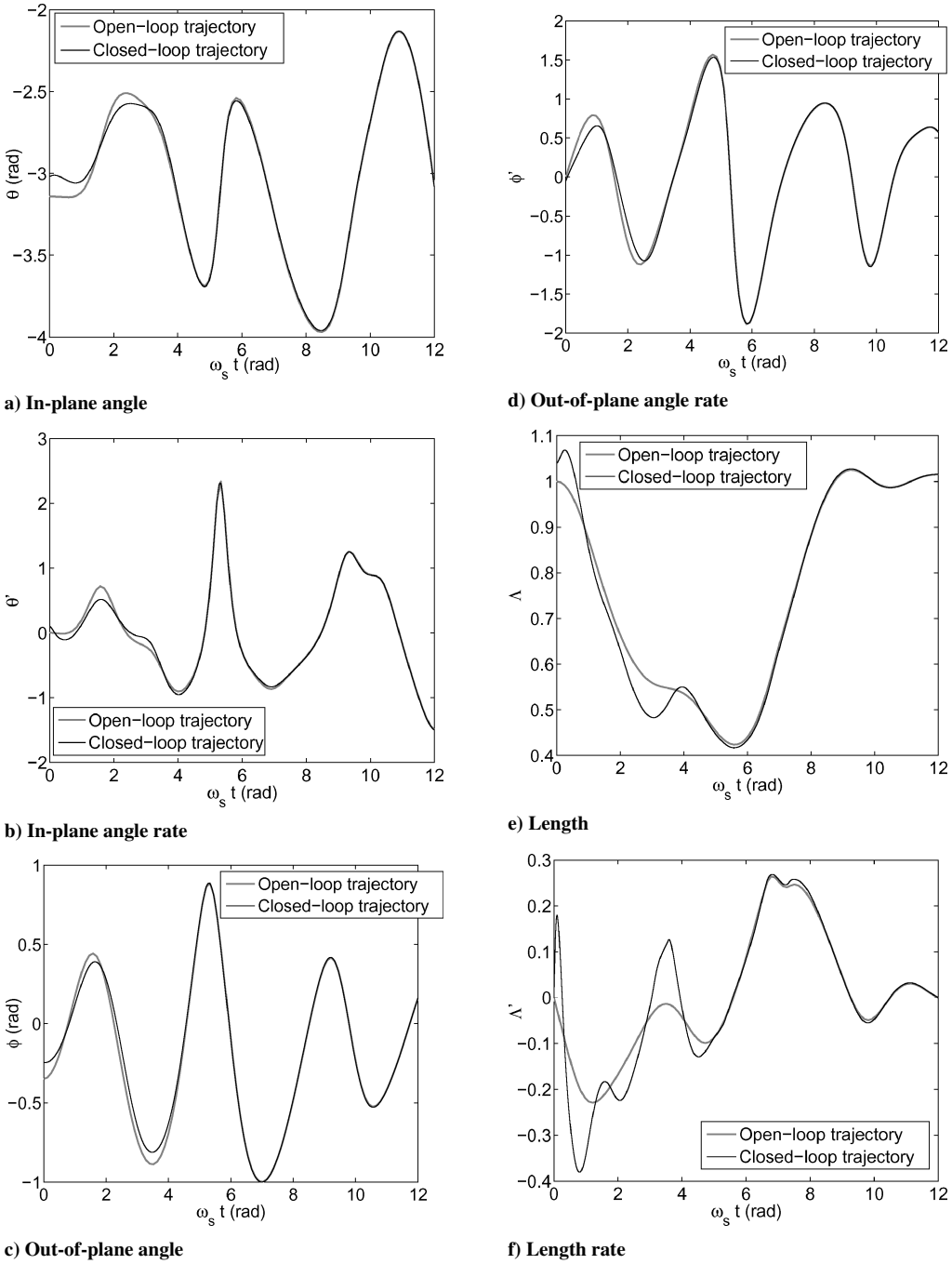

Fig. 5 Trajectories for 0.5-deg case.

that the tension saturates at the lower limit on two occasions for each of the cases. The lower limit on tension might pose a problem for a flexible tether because parts of the tether could become slack. Further study should be undertaken to determine how clipping the tension at different lower limits impacts the lateral oscillations of a flexible tether. For the 0.5-deg case, the maximum tension is on the order of 300 N and increases to approximately 400 N for the 1.5-deg case. As the inclination increases, the control tension is clipped at the lower limit for longer periods of time, which also explains why the higher inclination cases are more difficult to track using the receding horizon controller. Overall, the closed-loop control for all cases is excellent, despite relatively large perturbations to the initial conditions and changes to the subsatellite mass. The results also show that closed-loop control is possible with negligible assistance from the out-of-plane thruster. It is clear from the results presented for the three different cases that it is possible to effect significant changes to the three-dimensional motion of the tether tip using only tension control. It is also possible to achieve three different terminal states from the same set of initial conditions in under two orbits.

VII. Issues for Capture and Postcapture

The numerical results presented in the preceding section illustrate that it is possible to manipulate the motion of a long tether in three dimensions to achieve a fixed terminal state in under two orbits. In addition, it was shown that control around the nominal trajectory can be achieved using a combination of tension and minimal thruster control. However, many practical issues still remain if such a system is to be implemented. These are listed and discussed as follows:

A. Tether Flexibility

In this study, a relatively simple model of the tether has been used that neglects the tether flexibility. Inevitably, a real tether has

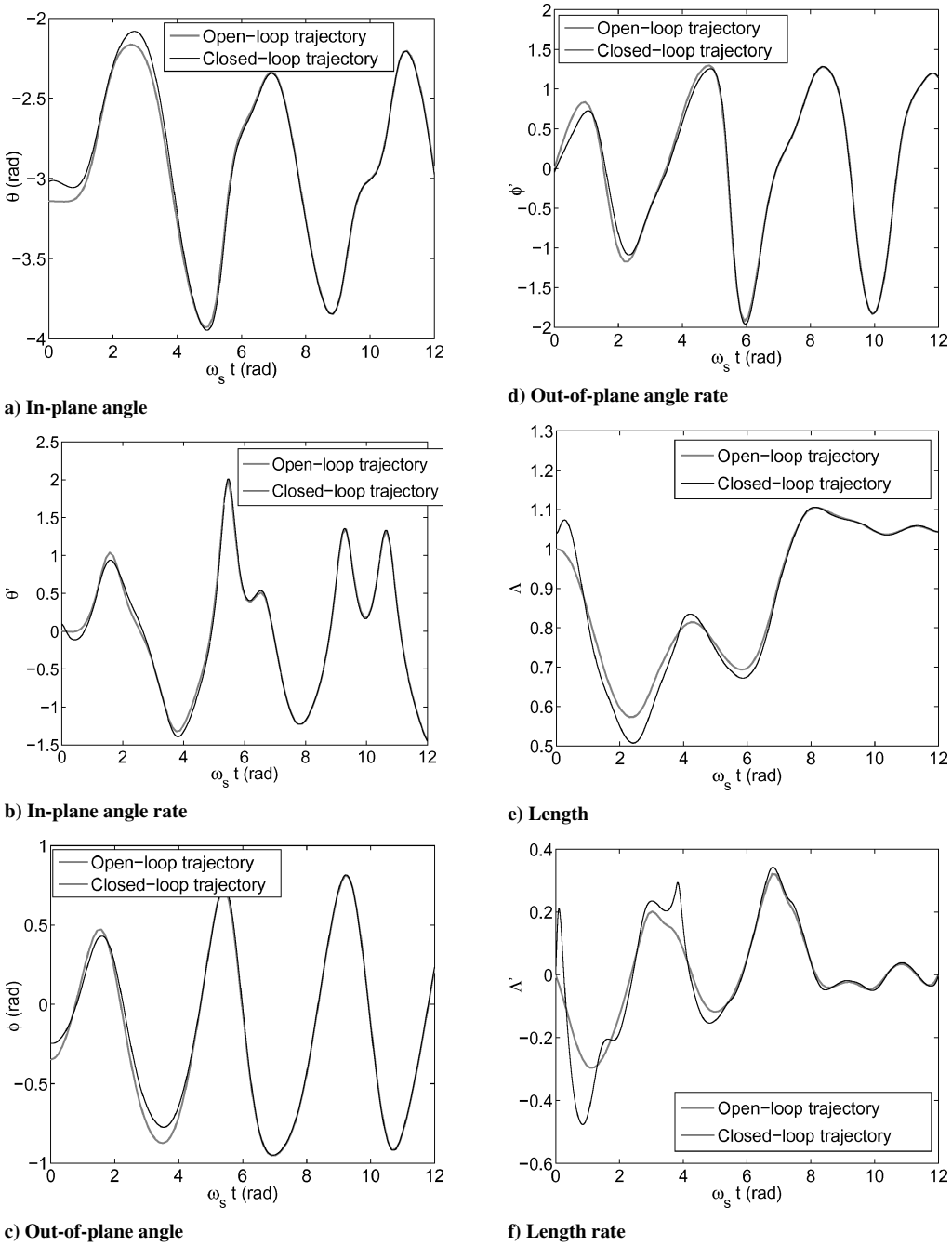

Fig. 6 Trajectories for 1.0-deg case.

both longitudinal and lateral vibrations that are coupled in both the in- and out-of-plane directions. Lateral modes can be important when trying to estimate the tether length or when measuring the tether tension at the deployer. However, their most important influence will be on the coupling with the longitudinal modes, that is, the distance to the tether tip tends to shorten due to the geometric bending of the tether. Further work is necessary to determine how much of an impact these dynamics will play on rendezvous.

B. Orbit Perturbations

This study assumed simple Keplerian orbits for the tether platform and payload and neglected the influence of the position of the center of mass of the tether system, that is, the system center of mass coincides with the tether platform. In reality, the actual position of the center of mass will vary relative to the tether platform due to the variation in tether length. This, together with the libration/orbit coupling, impacts the orbital motion of the system. If the tether platform mass is extremely large, this effect will be quite small, but it should be included in more detailed studies, particularly if this assumption does not hold. More important effects will be orbit perturbations due to Earth oblateness J_2, atmospheric drag, radiation pressure, etc. High-precision orbit propagation software and models should be used to assess the impact on the overall capture scenario.

C. Precision Position Rendezvous

The results presented here show that it is possible to achieve close proximity with the payload at the rendezvous time. However, it is not yet established that a precise match of the tether tip position and payload can be achieved. For example, it may be necessary to employ an additional controller in the vicinity of the rendezvous point that uses thrusters to guide the tip to the rendezvous position with precision. Several possibilities, such as employing a detachable

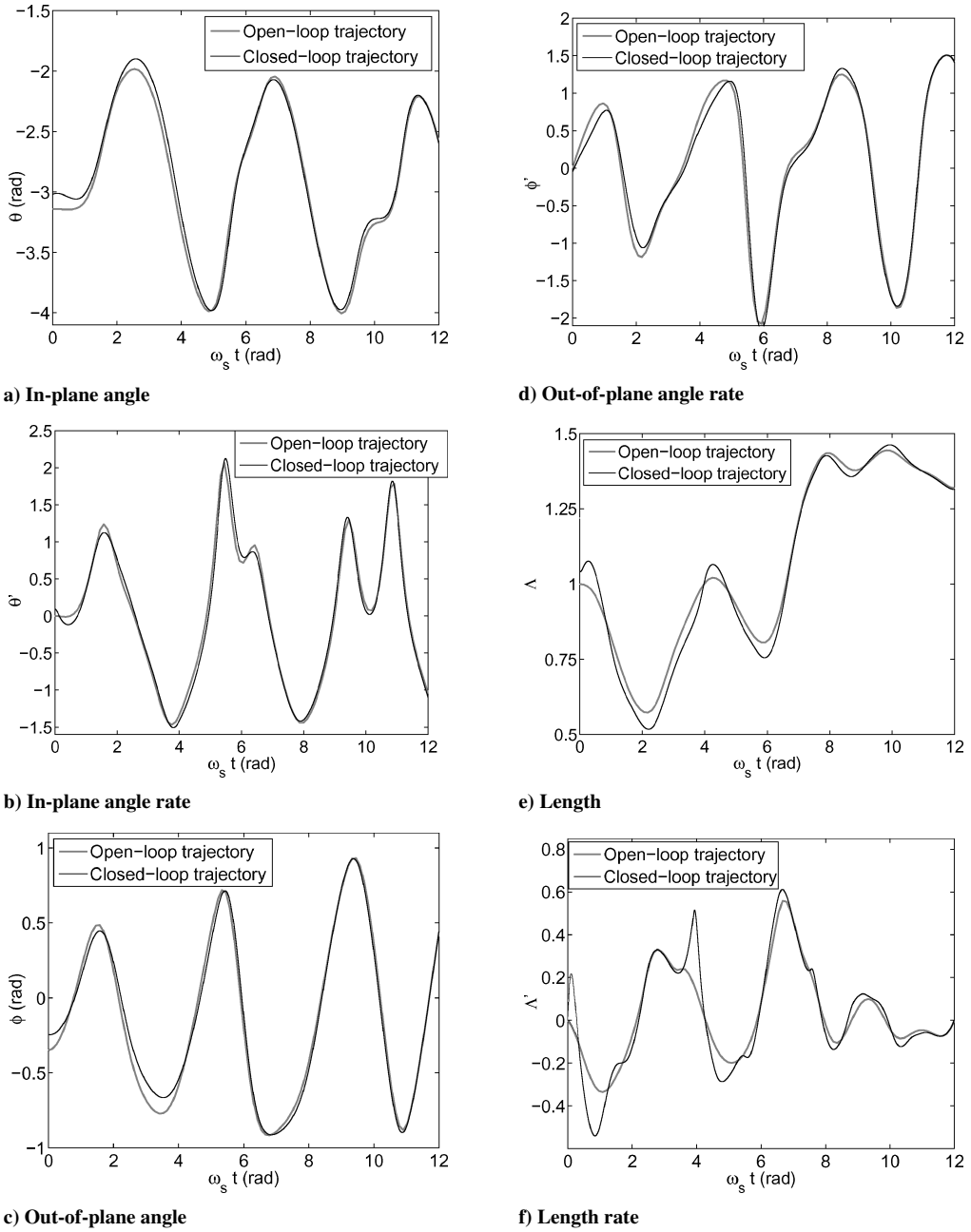

Fig. 7 Trajectories for 1.5-deg case.

maneuverable tip vehicle (tethered to the tether tip), have been suggested.[51]

D. Prolonged Rendezvous

This paper has considered only guiding the tether tip to the rendezvous location, but has given no consideration to the length of time the payload and tether tip are in close proximity. It is unlikely that gentle rendezvous will occur at a precise instant, and, therefore, methods for prolonging the rendezvous time should be investigated. Williams and Blanksby[52] studied a method for prolonging rendezvous using an additional mass that crawls along the tether to provide an extra degree of freedom for control. Proximity within 1 m for approximately 9 min is possible for in-plane capture using this method. The possibility of extending this approach to the three-dimensional case should be considered. Other possibilities, such as matching position and velocity at an instant and then releasing the tether tension may also be possible. However, practical considerations for how to recover control of the system would need to be investigated.

E. Capture with Significant Velocity Errors

The major consideration for achieving rendezvous is matching the positions of payload and tether tip. In some scenarios, errors in velocity may be permissible, but the resulting impulse at the tether tip introduces lateral traveling waves along a flexible tether. In this case, it is possible to damp the lateral vibrations by using a wave-absorbing controller, as first discussed by Fujii et al.[53] and further developed by Williams et al.[54]

F. Longitudinal Tension Waves

When a payload is captured at the tether tip, there is a sudden change in tension that propagates along the tether due to the mass added at the tether tip. This can set up high-frequency longitudinal vibration modes that could cause the tether to become slack, particularly when coupled with large amplitude librations. Methods for damping such effects have been developed by Colombo,[9] Carroll,[24] and Hoyt.[51]

The considerations just discussed are nontrivial. The possibility of incorporating all of the considerations into a unified controller should be the subject of future investigation.

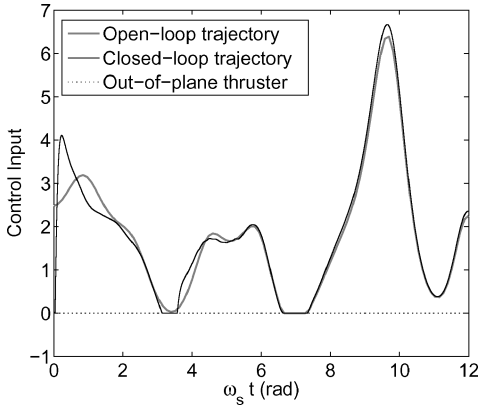

a) 0.5 deg

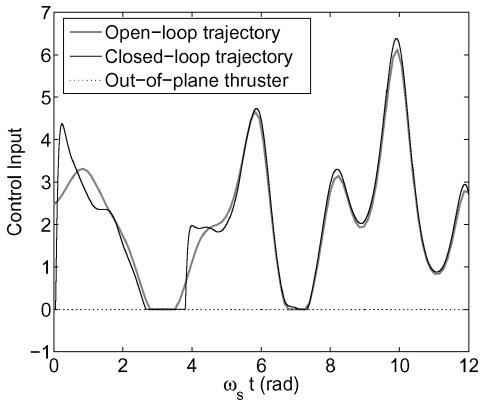

b) 1.0 deg

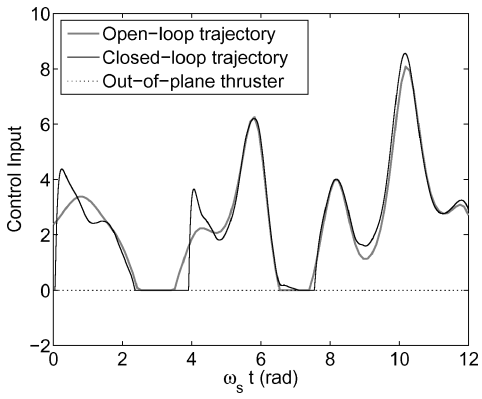

c) 1.5 deg

Fig. 8 Control inputs.

VIII. Conclusions

The possibility of using long tethers connected to a tether platform for capturing noncooperative payloads when there is a small relative inclination between their orbits is studied. When the tether length is limited to a maximum allowable length, capture opportunities tend to cluster around the point where the orbits intersect, particularly as the relative inclination between the orbits increases. An approach for generating an open-loop trajectory with a massive rigid tether model using tension control is developed by employing direct transcription. Rather than using collocation of the tension directly, a commanded tether length is introduced as a new control variable. Solutions for the problems studied in this paper are obtained using different initial guesses. Trajectories for three relative inclinations, 0.5, 1.0, and 1.5 deg show that it is possible to effect significant changes to the three-dimensional motion of the tether tip in under two orbits using only tension control. A nonlinear receding horizon feedback controller is used to simulate numerically the control of the system with large disturbances to the initial conditions and with changes to the system mass distribution. Several areas for further work should include simulating control laws in models that account for tether flexibility and orbital perturbations.

References

[1]Cosmo, M. L., and Lorenzini, E. C., *Tethers in Space Handbook*, 3rd ed., Smithsonian Astrophysical Observatory, Cambridge, MA, 1997.

[2]Misra, A. K., and Modi, V. J., "A Survey on the Dynamics and Control of Tethered Satellite Systems," *Advances in the Astronautical Sciences*, Vol. 62, 1987, pp. 667–719.

[3]Longuski, J. M., Puig-Suari, J., and Mechalas, J., "Aerobraking Tethers for the Exploration of the Solar System," *Acta Astronautica*, Vol. 35, No. 2, 1995, pp. 205–214.

[4]Johnson, L., Estes, R. D., Lorenzini, E. C., Martinez-Sanchez, M., Sanmartin, J., and Vas, I., "Electrodynamic Tethers for Spacecraft Propulsion," AIAA Paper 98-0983, Aug. 1998.

[5]Zimmerman, F., Schottle, U. M., and Messerschmid, E., "Optimal Deployment and Return Trajectories for a Tether-Assisted Re-Entry Mission," AIAA Paper 99-4168, Aug. 1999.

[6]Andres, Y. N., Zimmerman, F., and Schottle, U. M., "Optimization and Control of the Early Deployment Phase During a Tether Assisted Deorbit Maneuver," *Proceedings of the 22nd International Symposium on Space Technology and Science*, Japan Society for Aeronautical and Space Sciences and 22nd ISTS Organizing Committee, Tokyo, 2000, pp. 1795–1800.

[7]Williams, P., Blanksby, C., and Trivailo, P., "Optimal Control of Flexible Tethers," International Astronautical Congress, Paper IAC-03-A.6.05, AIAA, Reston, VA, Sept.–Oct. 2003.

[8]Moravec, H., "A Non-Synchronous Orbital Skyhook," *Journal of the Astronautical Sciences*, Vol. 25, No. 4, 1977, pp. 307–322.

[9]Colombo, G., "The Study of the Use of Tethers for Payload Orbital Transfer," NASA CR-170714, Smithsonian Astrophysical Observatory, Cambridge, MA, March 1982.

[10]Bekey, I., "Tethers Open New Space Options," *Astronautics and Aeronautics*, Vol. 21, April 1983, pp. 32–40.

[11]Bekey, I., and Penzo, P. A., "Tether Propulsion," *Aerospace America*, Vol. 24, July 1986, pp. 40–43.

[12]Wiesel, W. E., "Optimal Payload Lofting with Tethers," *Journal of Guidance, Control, and Dynamics*, Vol. 11, No. 4, 1988, pp. 352–356.

[13]Kyroudis, G. A., and Conway, B. A., "Advantages of Tether Release of Satellites from Elliptic Orbits," *Journal of Guidance, Control, and Dynamics*, Vol. 11, No. 5, 1988, pp. 441–448.

[14]Tillotson, B., "Spinning Tethers for Rapid Orbital Plane Change," *Proceedings of Space Technology and Applications International Forum (STAIF-2001)*, edited by M. S. El-Genk, CP 552, American Inst. of Physics, Melville, NY, 2001, pp. 519–524.

[15]Forward, R. L., "Tether Transport from LEO to the Lunar Surface," AIAA Paper 91-2322, July 1991.

[16]Nordley, G. D., and Forward, R. L., "Mars–Earth Rapid Interplanetary Tether Transport System. I: Initial Feasibility Analysis," *Journal of Propulsion and Power*, Vol. 17, No. 3, 2001, pp. 499–507.

[17]Westerhoff, J., "Optimal Configuration of MXER Tether Systems," AIAA Paper 2003-5220, Aug. 2003.

[18]Sorensen, K., "Hyperbolic Injection Issues for MXER Tethers," AIAA Paper 2003-5221, Aug. 2003.

[19]Hoyt, R. P., and Uphoff, C., "Cislunar Tether Transport System," *Journal of Spacecraft and Rockets*, Vol. 37, No. 2, 2000, pp. 177–186.

[20]Lorenzini, E. C., Cosmo, M. L., Kaiser, M., Bangham, M. E., Vonderwell, D. J., and Johnson, L., "Mission Analysis of Spinning Systems for Transfers from Low Orbits to Geostationary," *Journal of Spacecraft and Rockets*, Vol. 37, No. 2, 2000, pp. 165–172.

[21]Taylor, J., "Analysis and Issues of Conducting a Momentum Exchange Mission," AIAA Paper 2002-1125, Aug. 2002.

[22]Ziegler, S. W., and Cartmell, M. P., "Using Motorized Tethers for Payload Orbital Transfer," *Journal of Spacecraft and Rockets*, Vol. 38, No. 6, 2001, pp. 904–913.

[23]Carroll, J. A., "Tether Applications in Space Transportation," *Acta Astronautica*, Vol. 13, No. 4, 1986, pp. 165–174.

[24]Carroll, J. A., "Preliminary Design for a 1 Km/Sec Tether Transport Facility," NASA Office of Aeronautics and Space Technology, Third Annual Advanced Propulsion Workshop, Jan. 1992.

[25]Stuart, D. G., "Guidance and Control for Cooperative Tether-Mediated Orbital Rendezvous," *Journal of Guidance, Control, and Dynamics*, Vol. 13, No. 6, 1990, pp. 1102–1113.

[26]Blanksby, C., and Trivailo, P., "Assessment of Actuation Methods for Manipulating Tip Position of Long Tethers," *Space Technology, Space Engineering, Telecommunication, Systems Engineering and Control*, Vol. 20, No. 1, 2001, pp. 31–40.

[27]Williams, P., Blanksby, C., Trivailo, P., and Fujii, H. A., "Receding Horizon Control of Tether System Using Quasilinearisation and Chebyshev Pseudospectral Approximations," American Astronautical Society, Paper AAS 03-535, Aug. 2003.

[28]Westerhoff, J., "Active Control for MXER Tether Rendezvous Maneuvers," AIAA Paper 2003-5218, Aug. 2003.

[29]Lorenzini, E. C., Bortolami, S. B., Rupp, C. C., and Angrilli, F., "Control and Flight Performance of Tethered Satellite Small Expendable Deployment System-II," *Journal of Guidance, Control, and Dynamics*, Vol. 19, No. 5, 1996, pp. 1148–1156.

[30]Barkow, B., Steindl, A., Troger, H., and Weidemann, G., "Various Methods of Controlling the Deployment of a Tethered Satellite," *Journal of Vibration and Control*, Vol. 9, No. 1, 2003, pp. 187–208.

[31]Betts, J. T., "Survey of Numerical Methods for Trajectory Optimization," *Journal of Guidance, Control, and Dynamics*, Vol. 21, No. 2, 1998, pp. 193–207.

[32]Kirk, D., *Optimal Control Theory: An Introduction*, Prentice–Hall, Upper Saddle River, NJ, 1970.

[33]Morrison, D. D., Riley, J. D., and Zanzanaro, J. F., "Multiple Shooting Method for Two-Point Boundary Value Problems," *Communications of the ACM*, Vol. 5, No. 12, 1962, pp. 613, 614.

[34]Miele, A., "Recent Advances in Gradient Algorithms for Optimal Control Problems," *Journal of Optimization Theory and Applications*, Vol. 17, Dec. 1975, pp. 361–430.

[35]Lasdon, L. S., Mitter, S. K., and Waren, A. D., "The Conjugate Gradient Method for Optimal Control Problems," *IEEE Transactions on Automatic Control*, Vol. AC-12, No. 2, 1967, pp. 132–138.

[36]Ohtsuka, T., and Fujii, H. A., "Stabilized Continuation Method for Solving Optimal Control Problems," *Journal of Guidance, Control, and Dynamics*, Vol. 17, No. 5, 1994, pp. 950–957.

[37]Hargraves, C. R., and Paris, S. W., "Direct Trajectory Optimization Using Nonlinear Programming and Collocation," *Journal of Guidance, Control, and Dynamics*, Vol. 10, No. 4, 1987, pp. 338–342.

[38]Betts, J. T., *Practical Methods for Optimal Control Using Nonlinear Programming*, Society for Industrial and Applied Mathematics, Philadelphia, 2001.

[39]Elnagar, G., Kazemi, M. A., and Razzaghi, M., "The Legendre Pseudospectral Method for Discretizing Optimal Control Problems," *IEEE Transactions on Automatic Control*, Vol. 40, No. 10, 1995, pp. 1793–1796.

[40]Ross, I. M., and Fahroo, F., "Legendre Pseudospectral Approximations of Optimal Control Problems," *Lecture Notes in Control and Information Sciences*, Vol. 295, Springer-Verlag, Berlin, 2003, pp. 327–342.

[41]Melton, R. G., "Comparison of Direct Optimization Methods Applied to Solar Sail Problems," *Proceedings of the AIAA/AAS Astrodynamics Specialist Conference*, AIAA, Reston, VA, 2002, pp. 641–646.

[42]Josselyn, S., and Ross, I. M., "Rapid Verification Method for the Trajectory Optimization of Reentry Vehicles," *Journal of Guidance, Control, and Dynamics*, Vol. 26, No. 3, 2003, pp. 505–508.

[43]Williams, P., "Optimal Control of Tethered Planetary Capture Missions," *Journal of Spacecraft and Rockets*, Vol. 41, No. 2, 2004, pp. 315–319.

[44]Monshi, N., Misra, A., and Modi, V. J., "On the Reel Rate Control of Retrieval Dynamics of Tethered Satellite Systems," *Proceedings of the AAS/AIAA Spaceflight Mechanics Meeting*, Univelt, San Diego, CA, 1991, pp. 1053–1075.

[45]Betts, J. T., and Gablonsky, J. M., "A Comparison of Interior Point and SQP Methods on Optimal Control Problems," Boeing Phantom Works, Mathematics and Computing Technology, Rept. M&CT-TECH-02-004, Seattle, WA, March 2002.

[46]Betts, J. T., and Huffman, W. P., "Sparse Optimal Control Software—SOCS," Mathematics and Engineering Analysis Library, Rept. MEA-LR-085, Boeing Information and Support Services, Seattle, WA, 1997.

[47]Gill, P. E., Murray, W., and Saunders, M. A., "SNOPT: An SQP Algorithm for Large-Scale Constrained Optimization," *SIAM Journal of Optimization*, Vol. 12, No. 4, 2002, pp. 979–1006.

[48]Bryson, A. E., *Dynamic Optimization*, Addison Wesley Longman, New York, 1999, Chap. 8.

[49]Yan, H., Fahroo, F., and Ross, I. M., "Real-Time Computation of Neighbouring Optimal Control Laws," AIAA Paper 2002-4657, Aug. 2002.

[50]Williams, P., "Application of Pseudospectral Methods for Receding Horizon Control," *Journal of Guidance, Control, and Dynamics*, Vol. 27, No. 2, 2004, pp. 310–314.

[51]Hoyt, R. P., "Moon & Mars Orbiting Spinning Tether Transport Architecture Study," Final Rept., NASA Inst. for Advanced Concepts, NIAC Phase 2 Contract 07600-034, Aug. 2001.

[52]Williams, P., and Blanksby, C., "Prolonged Payload Rendezvous Using a Tether Actuator Mass," *Journal of Spacecraft and Rockets*, Vol. 41, No. 5, 2004, pp. 889–892.

[53]Fujii, H. A., Watanabe, T., Taira, W., and Trivailo, P., "An Analysis of Vibration and Wave-Absorbing Control of Tether Systems," AIAA Paper 2001-4033, Aug. 2001.

[54]Williams, P., Watanabe, T., Blanksby, C., Trivailo, P., and Fujii, H. A., "Libration Control of Flexible Tethers Using Electromagnetic Forces and Moveable Attachment," *Journal of Guidance, Control, and Dynamics*, Vol. 27, No. 5, 2004, pp. 882–897.

D. Spencer
Associate Editor